# CHAOS IN THE POST-NEWTONIAN GRAVITATIONAL THREE-BODY PROBLEM

by

JJ Campbell

Physics 492R Capstone Project Report

Also submitted to Brigham Young University in partial fulfillment

of graduation requirements for University Honors

Department of Physics and Astronomy

December 2008

Advisor: David Neilsen Honors Representative: Bruce Collings

Signature: _____ Signature: _____

BRIGHAM YOUNG UNIVERSITY

DEPARTMENT APPROVAL

of a honors thesis submitted by

JJ Campbell

This thesis has been reviewed by the research advisor, research coordinator, and department chair and has been found to be satisfactory.

| | |
|---|---|
| Date | David Neilsen, Advisor |
| Date | Branton Campbell, Research Coordinator |
| Date | Ross L. Spencer, Chair |

ABSTRACT

# CHAOS IN THE POST-NEWTONIAN GRAVITATIONAL THREE-BODY PROBLEM

JJ Campbell

Department of Physics and Astronomy

Bachelor of Science

In classical Newtonian gravity, the three-body problem is known to be chaotic for general initial data. We investigate the existence of chaos for the three-body problem in general relativity using the first post-Newtonian approximation. Our initial data consists of a third object entering a binary pair and is parameterized by an impact parameter and phase angle. The Hamiltonian equations of motion are integrated using adaptive methods and we extract gauge-independent quantities at infinity. We present results that characterize chaos in general relativity.

# ACKNOWLEDGMENTS

First of all, I want to thank my advisor, Dr. David Neilsen. His patience in teaching me not only what to do, but what it was that I was doing, helped me to truly be excited about this project. I would also like to thank David Tanner whose work we have been extending. Thanks to Miriam Conde for her collaboration and help. For financial assistance I owe thanks to the Physics Department of BYU, NSF grant PHY-0653389, an ORCA grant, and the Heritage Scholarship from BYU. One friend who has spent countless hours assisting my research is Marylou4, the supercomputer here at BYU. Without her this would have been impossible. Of course, a big thanks to my family as well. Their love and encouragement have molded my character and helped teach me the value of work and the joy of striving for the impossible. Thank you to everyone else who has helped me to get this done and all who appreciates what they read here.

# Contents

# List of Figures

# Chapter 1

# Introduction

## 1.1 Why?

In a galaxy far far away there is a planetary system very much like ours. This system cannot be easily modeled because there happens to be this very large planet that seems to affect the orbits of the other objects orbiting the central star. A rough approximation using only two bodies, namely the star and any orbiting body of interest, can give some good basic information about what is going on. Some phenomena are not so readily explained with this simplified model though. There appear to be some gaps in an asteroid belt for example. In our Solar System these gaps in the asteroids were explained by increasing the fidelity of the model to include Jupiter as a third interacting body and then solving what has come to be known as the restricted three body problem [1].

Our Solar System is even more complex than just a three body problem, but just as the two body problem provided a good approximation in the time of Newton and Keppler, we now use the three body problem as an approximation to learn about other phenomena. Understanding complex interactions becomes even more interesting as we

look deep into space and see star clusters, galaxies, and begin to find other planetary star systems. Another place to see some good examples is the microscopic world, more specifically the atomic and subatomic levels.

One of the intriguing things about the classical gravitational three body problem is that it is inherently chaotic. With only two bodies a closed solution is available and it is easy to determine what would happen to a system for any given situation. With three bodies a general solution can only be found numerically. Moreover, if the problem is chaotic, then solutions that differ by $\frac{1}{1000}$ the radius of one of the bodies in your initial positioning will give very different answers.

Returning to the Solar System and to stars in general there is another simplification I would like to touch on. Newton's model of gravity is a force that draws massive objects together. His equations did not quite explain everything though. The planets seem to have trouble staying in simple elliptical orbits. They like to make their orbits precess just a little bit and after millions of years a sketch of their path would look more like a flower than a single petal. Einstein's theory of relativity, while not derived to explain this, calculated the observed precession of the planets.

People are now working to combine relativity and multi body motion. Before beginning that, let us take a step back and explain a little more about some of the important components of this study. The three elements that will be most important here are chaos, relativity, and the three-body problem.

## 1.2 What is Chaos?

As used in physics, "chaos" refers to an extreme sensitivity to initial conditions. This sensitivity is measured by comparing two solutions in phase space with nearly identical initial conditions. Let the initial points in phase space for two solutions

differ by a small amount $\delta\mathbf{x}\,(0)$ and the separation at time $t$ be $\delta\mathbf{x}\,(t)$. If the system is chaotic, then $\delta\mathbf{x}\,(t)$ will grow exponentially in time according to

$$|\delta\mathbf{x}\,(t)\,| \approx e^{\lambda t}|\delta\mathbf{x}\,(0)\,| \tag{1.1}$$

where $\lambda$ represents the Lyapunov exponent, or a measure of the mean rate of separation [2]. If $\lambda$ is negative then $\delta\mathbf{x}\,(t)$ will go to 0 and there is no chaos. If $\lambda$ is positive then the system is chaotic.

This extreme sensitivity to initial conditions is sometimes called the "butterfly effect". This common phrase takes its name from weather patterns where a small change in atmospheric conditions, the equivalent of the flap of a butterfly's wings, can set off a chain of events creating a tornado that hits Chicago. This same flap of the butterfly's wings, if done a fraction of a second later, could prevent the formation of a massive blizzard across the Midwest. This phenomenon makes predicting weather difficult, but it applies to a number of other common occurances. Traffic patterns, bacterial growth, spread of disease, the flocking behavior of Starlings, coupled oscillators, economic trends, and even purchasing behavior are all modeled with non-linear differential equations. This means that in all but a few special cases you need a supercomputer and very intense numerical calculations to get an accurate model.

Another common trait found in chaotic systems is self-similarity, or scale invariance. This would be like looking at a forest, and then when you got closer finding out that each tree was really just a bundle of sticks. Looking closer, each of those sticks is really a collection of smaller sticks. The smaller sticks, upon closer investigation, appear to be made entirely of lashed toothpicks. At each level the structure is similar, and as you continue to get closer you find that the same patterns keep repeating.

## 1.3 The Role of Relativity

When dealing with stellar and planetary motions, Newtonian Mechanics gives good approximations to what we observe. General relativity gives a much more accurate model, but is computationally time intensive, even for a supercomputer. Sometimes, corrections can be made to the Newtonian model to improve the accuracy that are good enough to be interesting, but do not carry quite the processing cost.

General relativity is a model of the universe with curved space-time. To illustrate curvature effects in two dimensions, imagine a globe. On the surface of the globe, the shortest distance between two points is the *geodesic*. From the perspective of an ant on the globe, the geodesic is a straight line. From the three dimensional view of the globe, the geodesic curves making a circular arc. In four dimensions, all of space-time is curved in complex ways that make something that appears flat to us a veritable piece of abstract art. This curving is done by objects with mass and energy. Going back to two dimensions, imagine all of space being a giant rubber sheet with marbles of varying sizes on it to represent planets, stars, and other massive bodies. Extend that concept in two more dimensions and that is how general gelativity percieves the universe.

To do calculations with full general relativity requires the use of non-linear partial differential equations. This is a fancy way to say "really hard math". It is now possible to run the full general relativistic equations for multiple bodies [3], but to run simulations with such math is computationally intense and therefore impractical for the millions of simulations needed for the comparisons in the chaos that we present here. It is possible to derive a simplified form of the equations that are valid when $\frac{v^2}{c^2} \ll 1$ and $|\Phi| \ll 1$ where $\Phi = \frac{Gm_1m_2}{r}$ [4]. These simplified equations are a perturbative expansion known as the post-Newtonian, or PPN, equations. To get some

insight into the effects of relativity on the chaos in the general three-body problem we will here use the PPN1, or first order post-Newtonian gravity.

## 1.4 Three Bodies

The three body gravitational problem is an example of a deterministically chaotic problem, or a chaotic problem whose final solution can be calculated if the initial conditions are known with infinite precision. With two bodies, the motion is simple and it is possible to solve the system analytically. With three or more bodies, analytic solutions are generally impossible to find, except in some special cases [5].

The number of three-body interactions in our universe is staggering. Looking up at the night sky only hints at the number of N-body interactions occurring between stars, galaxies, and planets. Zooming in to look at tiny particles, the ones invisible to even the best microscopes, similar multi-body interactions abound. Researching three-body interactions is an important step to being able to understand how stars, planets, and particles move. It even applies to the solar system. This means that the orbits of the planets can only be accurately modeled out to some tens of millions of years [6]. It also means that asteroids currently in seemingly stable orbits will aperiodically be sent on their ways [1] [6]. There is even a possibility, though slight it might be, that one of the planets could be ejected out of the system, or that one of them already has been [1].

Detailed calculations in the solar system require multiple bodies. The three body problem is a step in that direction that has applications not only to the solar system, but to space in general. The restricted three-body problem, or one in which two of the bodies are massive enough to allow the assumption that they are unaffected by the third body, has been of particular interest for things such as predicting the motion

of asteroids orbiting the sun at approximately the distance of Jupiter [1].

What we find is that with the removal of each simplification we find new explanations and new insight into reality. Most of the time these corrections are small. For example, the magnitude of the corrections that using the PPN1 formalism gives are tiny. When dealing with chaos however, particularly in astronomical time, the accumulated results of small corrections are important.

## 1.5 This Study

In this study we examine chaos in the relativistic three-body problem making comparisons between Newtonian and PPN1 gravity. Specifically, we are looking at how the Post-Newtonian corrections affect the results of simulated interactions. We start by reproducing some of the results found by Boyd and McMillan in 1993 on the Newtonian three-body problem [7]. We run simulations differing only in the equations used for gravity to then compare the effects of the relativistic corrections. In one case we use Newtonian gravity, and in the other we use the PPN1 gravity. We compare simulations with nearly identical initial condistions. When the final solutions are nearly identical, then chaotic effects are not apparent for these parameters. When the final solutions are significantly different then this indicates chaos. The simulations are graphed to show three variables, one on each of the axis and then one using a color gradient. Two variable initial conditions are plotted along the axis and one frame independent final variable is given a color value. The effects that are of particular interest include the fine structure (scale invariance), the transition between stable and chaotic results, and the extreme situations where the mathematical models break down and introduce errors. We also present work done to verify the accuracy of the program being used for the simulations.

# Chapter 2

# The Setup and Equations of Motion

## 2.1 Equations of Motion

Now that we know what we are going to do, the question is how. One effective way to deal with orbiting bodies is to use the Hamiltonian formalism. For Newtonian gravity this is fairly straight forward. The Hamiltonian for the Newtonian approximation of gravity is:

$$H = \frac{1}{2}\sum_a \frac{\boldsymbol{p}_a^2}{m_a} - \frac{1}{2}G\sum_a\sum_{b\neq a}\frac{m_a m_b}{r_{ab}}, \tag{2.1}$$

where the first term represents the summed rest energy of all of the masses, the second term is the sum of the kinetic energies, and the third sum is of the gravitational potential energies between each of the bodies. As you will be able to see in chapter 4 even this equation is nonlinear and leads to chaotic results. The Hamiltonian for

Einstein's PPN1 gravity is [8]:

$$\begin{aligned} H = & \sum_a m_a + \frac{1}{2}\sum_a \frac{\boldsymbol{p}_a^2}{m_a} - \frac{1}{2}G\sum_a\sum_{b\neq a}\frac{m_a m_b}{r_{ab}} - \frac{1}{8}\sum_a m_a\left(\frac{\boldsymbol{p}_a^2}{m_a^2}\right)^2 \\ & - \frac{1}{4}G\sum_a\sum_{b\neq a}\frac{m_a m_b}{r_{ab}}\left(6\frac{\boldsymbol{p}_a^2}{m_a^2} - 7\frac{\boldsymbol{p}_a\cdot\boldsymbol{p}_b}{m_a m_b} - \frac{(\boldsymbol{n}_{ab}\cdot\boldsymbol{p}_a)(\boldsymbol{n}_{ab}\cdot\boldsymbol{p}_b)}{m_a m_b}\right) \\ & + \frac{1}{2}G^2\sum_a\sum_{b\neq a}\sum_{c\neq a}\frac{m_a m_b m_c}{r_{ab}r_{ac}}. \end{aligned} \tag{2.2}$$

Here, $G$ is the gravitational constant, $m_a$ is the mass of body $a$, $\boldsymbol{p}_a$ is the momentum vector of body $a$, $r_{ab}$ is the magnitude of the position vector from body $a$ to body $b$, and $\boldsymbol{n}_{ab}$ is the unit vector along $\boldsymbol{r}_{ab}$. The equations of motion (or Hamilton's equations) are

$$\dot{q}_i = \frac{\partial H}{\partial p_i} \tag{2.3}$$

and

$$\dot{p}_i = \frac{\partial H}{\partial q_i}, \tag{2.4}$$

where $H$ is the Hamiltonian, $q_i$ is a generalized coordinate vector, $i$ is an index that ranges over the defining variables of all three bodies, and $p_i$ is the conjugate momentum.

There are 18 initial variables, three for position and three for momentum for each of three bodies. We use Maple to calculate the equations of motion and to generate Fortran code for all of the equations used in both the Newtonian and the PPN1 gravitational models. This code is then used to numerically simulate the motions of the three bodies.

## 2.2 It's a Setup

To examine chaos in the relativistic three body problem, I adopt an approach similar to that of Boyd and McMillan [7]. I begin with nearly identical initial conditions and

then compare the final outcomes to obtain a general idea of how the system evolves. Chaotic and non-chaotic regions should both be present. The chaotic regions should show different final outcomes with small changes in the initial conditions. The non-chaotic, or smooth, regions should have gradual change in the final outcomes as the initial conditions are modified.

To make this easier to study graphically we have also used Boyd and McMillan's strategy to limit the number of independent initial conditions to two [7]. Beginning with the 18 variables previously mentioned, we use the laws of conservation of energy, angular momentum, and linear momentum to remove four of the unknowns in our equations. We then simplify things a little bit more by constraining the motion to a plane so that $z = 0$ and $\boldsymbol{p}_z = 0$ for all three bodies. We further restrict the system by using a center of mass frame of reference. This leaves us with only a six-dimensional phase space. For greater simplicity we make the binary rotate in a circular pattern and fix the separation to $2a$, where $a$ is the radius of the binary. The distance to the third body, and all other relevant distances, are given in terms of $a$. Finally, we allow the binary to only orbit in the counter-clockwise direction. This finally reduces the number of independent initial conditions to two, a phase angle of the orbiting pair, and an impact parameter of the incoming body.

Figure 2.1 shows how these two parameters are used in this system. The two masses in the binary are designated bodies 1 and 2. The incoming is body 3. The parameters $\phi$ and $\rho$ are the phase angle and the impact parameter at the beginning of the simulations and are varied in small increments. The constants used for the simulations are:

$$m_1 = m_2 = m_3 = 1 \times 10^6 \mathrm{kg}, \tag{2.5}$$

$$G = 6.673 \times 10^{-11} \frac{\mathtt{m}^3}{\mathrm{kgs}^2}, \tag{2.6}$$

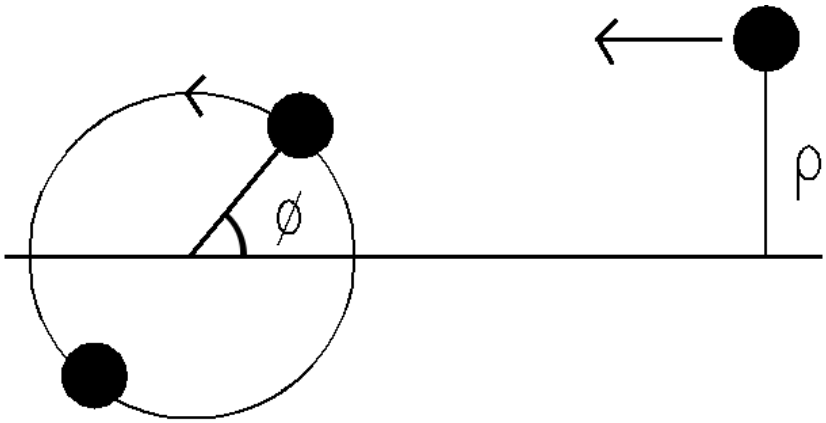


**Figure 2.1** 3 bodies, 2 in a bound orbit and 1 from infinity.

$$a = 0.1\text{m}. \tag{2.7}$$

The initial positions of the bodies are:

$$\mathbf{x}_1 = \left( \frac{am_2}{m_1 + m_2} \cos(\phi), \frac{am_2}{m_1 + m_2} \sin(\phi), 0 \right), \tag{2.8}$$

$$\mathbf{x}_2 = \left( -\frac{am_2}{m_1 m_2} \cos(\phi), -\frac{am_2}{m_1 m_2} \sin(\phi), 0 \right), \tag{2.9}$$

$$\mathbf{x}_3 = (60a, \rho, 0). \tag{2.10}$$

The equations for position 2.8 and 2.9 come from using the reduced mass and the phase angle to pinpoint the locations of the bodies. The position of the third body 2.10 is given at a far distance given as a multiple of $a$ and the impact parameter $\rho$ which we also make a multiple of $a$. The initial velocities are:

$$\mathbf{v}_1 = \left( -\frac{m_2}{m_1 + m_2} v \sin(\phi), \frac{m_2}{m_1 + m_2} v \cos(\phi), 0 \right), \tag{2.11}$$

$$\mathbf{v}_2 = \left( \frac{m_1}{m_1 + m_2} v \sin(\phi), -\frac{m_1}{m_1 + m_2} v \cos(\phi), 0 \right), \tag{2.12}$$

$$\mathbf{v}_3 = \left(-\frac{1}{2}v_c, 0, 0\right), \tag{2.13}$$

$$v = \sqrt{G\frac{m_1 + m_2}{a}}, \tag{2.14}$$

$$v_c = \sqrt{Gm_1\frac{m_1 + m_2 + m_3}{4am_3}}. \tag{2.15}$$

Equation 2.14 comes from the condition that the orbit is circular. The equation for $v_c$, Eq. 2.15, gives the critical velocity for body 3. This velocity is the threshold velocity for the incoming body above which the total energy of the system is positive. This is multiplied by a fraction to ensure that the total energy of the system is negative to allow for temporary bound states to occur [7]. The two initial conditions are then varied as

$$0 \leq \phi \leq 2\pi \tag{2.16}$$

and

$$-6.5a \leq \rho \leq 9a. \tag{2.17}$$

The simulations of each set of initial conditions are designed to end when one of the bodies is ejected from the system. At this point, we record which body escaped and the initial and final Hamiltonian values. These are recorded because of their invariance with frame of reference. Which body escaped allows us map the chaos, and the difference in the Hamiltonians gives us a way to assure that conservation laws are obeyed.

# Chapter 3

# Solving the Thing and Checking the Accuracy

## 3.1 The Paintbrush and the Strokes

We use computational methods to solve the equations of motion for the evolution of the system. By making graphs that focus on a single variable that is measured at the time of escape, or when one of the bodies is expelled from the system, we can visualize the results of thousands of simulations. In the next chapter some of these graphs will be shown and explained, but first I need to cover a bit of the methods used and the assumptions made in creating these images. If you are simply interested in the art and not in the types of brushes and the stroke techniques then I recommend leaping ahead to the next chapter.

## 3.2 LSODA

The three body gravitational problem is not only computationally intense, but it also requires a range of scales. There are times when the bodies are widely separated and then there are times when the bodies are close together. When they are separated, it is best to use large time steps and save the computation time. When they are close, small steps are necessary to ensure accuracy. This requires adaptivity in the solution method. We achieve this by using the Livermore Solver for Ordinary Differential equations, with Automatic method switching for stiff and non-stiff problems, or LSODA [9] as a part of our algorithm.

LSODA is an adaptive ODE solver that uses both the Adams-Moulton and Adams-Bashforth methods. LSODA adaptively adjusts the time steps and automatically switches methods for stiff and non-stiff problems. The time step size is determined using Richardson extrapolation. LSODA also requires a certain precision, or error tolerance, to be inputted as a measure for when it is "close enough".

## 3.3 Accuracy Verification

LSODA is the best solver available for this specific problem. I had to verify that it could handle these types of problems and find a threshold for where "close enough" really was close enough. Lacking any good theoretical model for a three-body problem on which to test LSODA, I tested it using the two-body problem, and the restricted three-body problem.

## 3.4 Testing LSODA

To verify the accuracy of LSODA I simplified the problem to a binary system and Newtonain gravity. This allowed me to check LSODA and the rest of our programs to make sure that our experiments matched theory. In Newtonian gravity a binary system is stable and there should be no precession or spiraling. By graphing the progress of a single simulation of a binary, and particularly by focusing on the first and last orbits, I tracked the changes in the orbits. I also extended the error check to the restricted three body problem, where the third body has a mass much less than the other two.

Fig. 3.1 shows the most simple test with a unequal mass binary with the orbiting body in a nearly circular orbit. The top of Fig. 3.1 has time graphed along the Z-axis to show how the orbit progresses over time, and then the bottom of Fig. 3.1 has only the first and the last orbit drawn in different colors to show how little the orbit changes over time. Due to the simple nature of this problem I considered only a little over 60 orbits to be sufficient. This still shows that in this case LSODA and the other programs are all working correctly. I did find that to prevent the orbit from collapsing I had to constrain the maximum error to $1x10^{-10}$.

Fig. 3.2 and Fig. 3.3 are similar to Fig. 3.1, but with progressively greater eccentricities. The first and last orbits are drawn with different colors as before and the maximum error is constrained to be $1x10^{-10}$. There is no rotation, deformation, or collapse of the orbits from which I conclude that the programs are working appropriately. Fig. 3.2 has over 10,000 orbits to verify that even over long periods the programs continue to function properly. Fig. 3.3 was more computationally demanding and so the number of orbits was reduced to just under 100. The drift in the y direction may be due to imperfect initial conditions with the velocity in the y

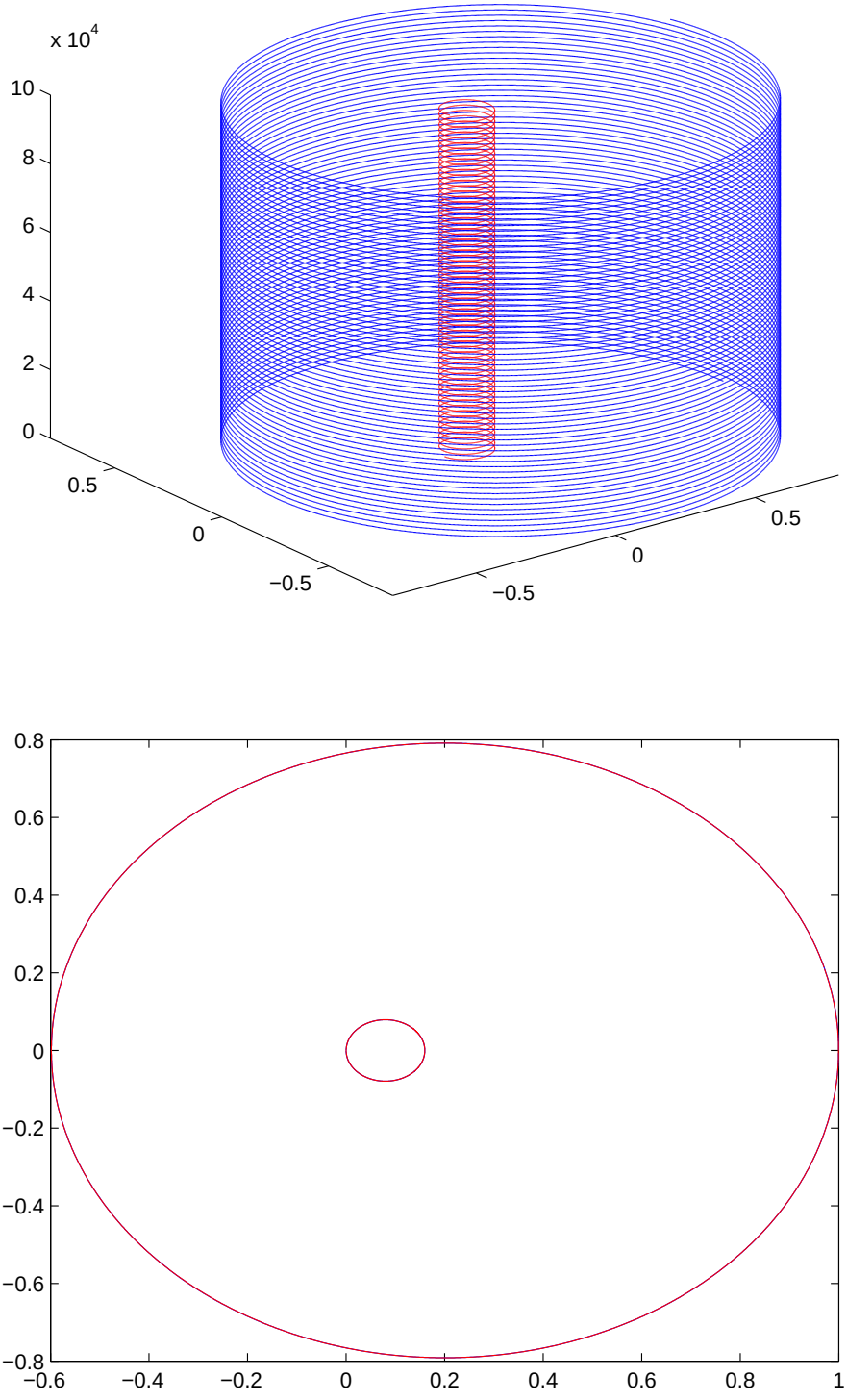


**Figure 3.1**
Top: test on LSODA of nearly circular binary orbit with time in Z.
Bottom: initial and final orbits of the aforementioned test as seen from above.

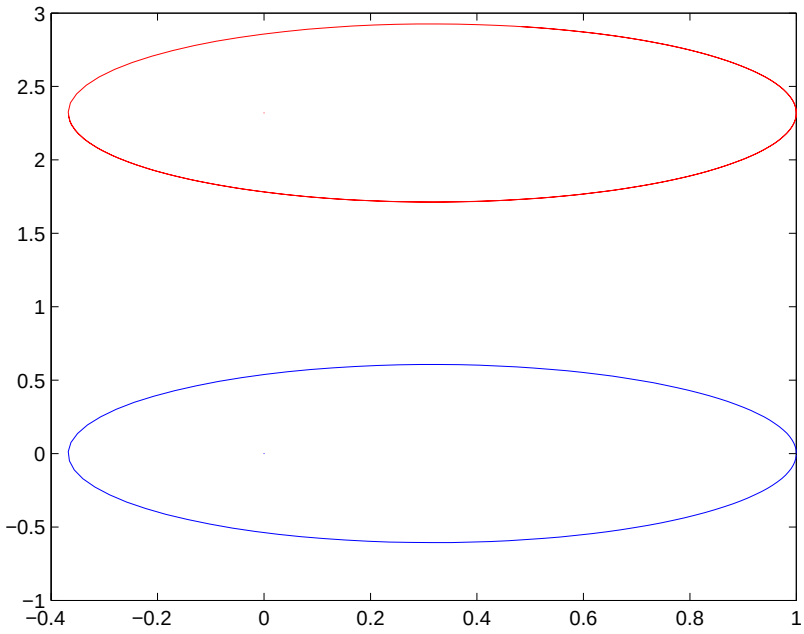


**Figure 3.2** View of the first and last orbits of an eccentric binary showing drift, but no deformation or rotation.

direction not quite equal to 0.

Fig. 3.4 shows the restricted three-body problem in Newtonian gravity. The 3D image has time on the Z-axis to show to the progression through time and the comparison picture has the initial orbits drawn using dashed lines and the final orbits drawn with solid lines. By constraining the error to $1x10^{-10}$ we once again see stable orbits that do not deform, although this simulation was only allowed to run for just under 20 orbits.

I took the evidence gathered here as sufficient to support our use of LSODA as an effective ODE solver for gravitational problems with the error tolerance appropriately limited to $1x10^{-10}$.

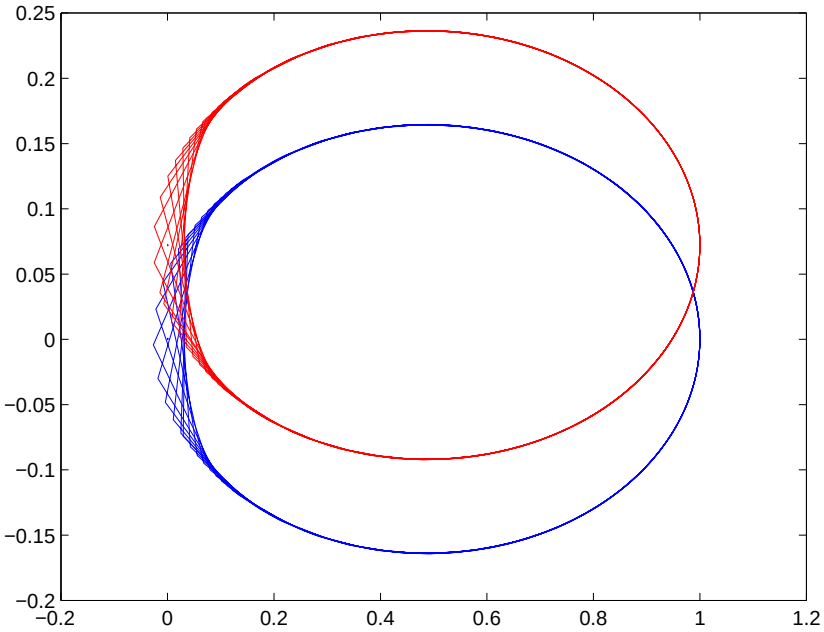


**Figure 3.3** The first few and last few orbits of a system with an extreme eccentricity showing drift, but stable in shape and orientation.

## 3.5 Hamiltonian Check

Since no good theoretical model exists to allow us to perform the above test for three-bodies, I wanted a second test to verify our results. Conservation laws provide such a check. Since our Hamiltonian is independent of time, it is a simple task to ask the computer to record the initial and final Hamiltonians and use them to check for conservation. I found that the initial an dfinal Hamiltonians typically varied by 1 part in $10^6$. To examine these conservations of the Hamiltonian in more detail consider figure 3.5.

The graphs will make more sense after reading the next chapter, but for now it is sufficient to look at the scale. In the two greenish figures, Fig. 3.5, the difference in the Hamiltonian from the beginning to the termination of each simulation is graphed. The top of Fig. 3.5 is of the Newtonain approximation and the bottom is of the PPN1

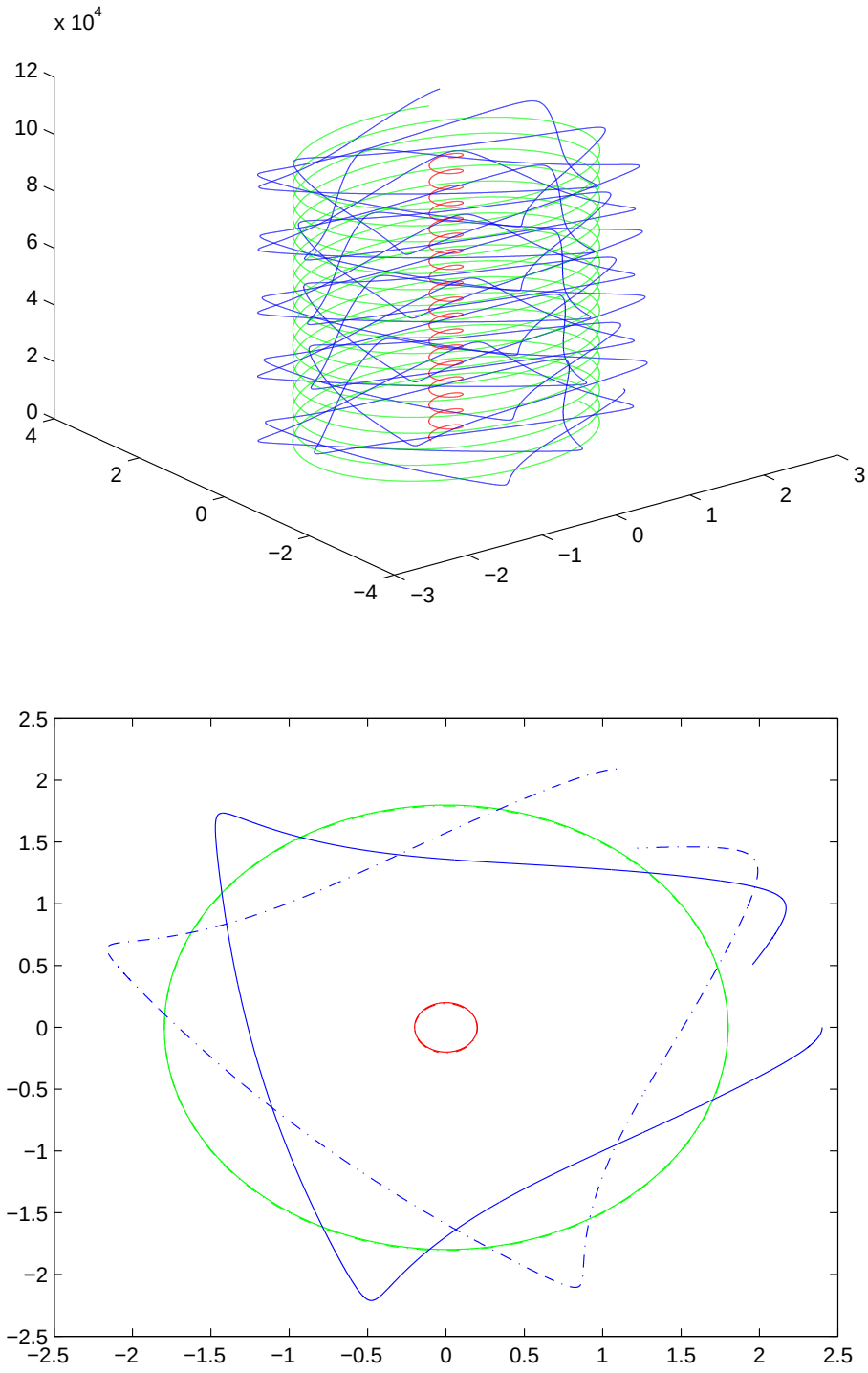


**Figure 3.4** Restricted three-body test against time (top) and with the initial orbits in dashes and final orbits in solid lines (bottom).

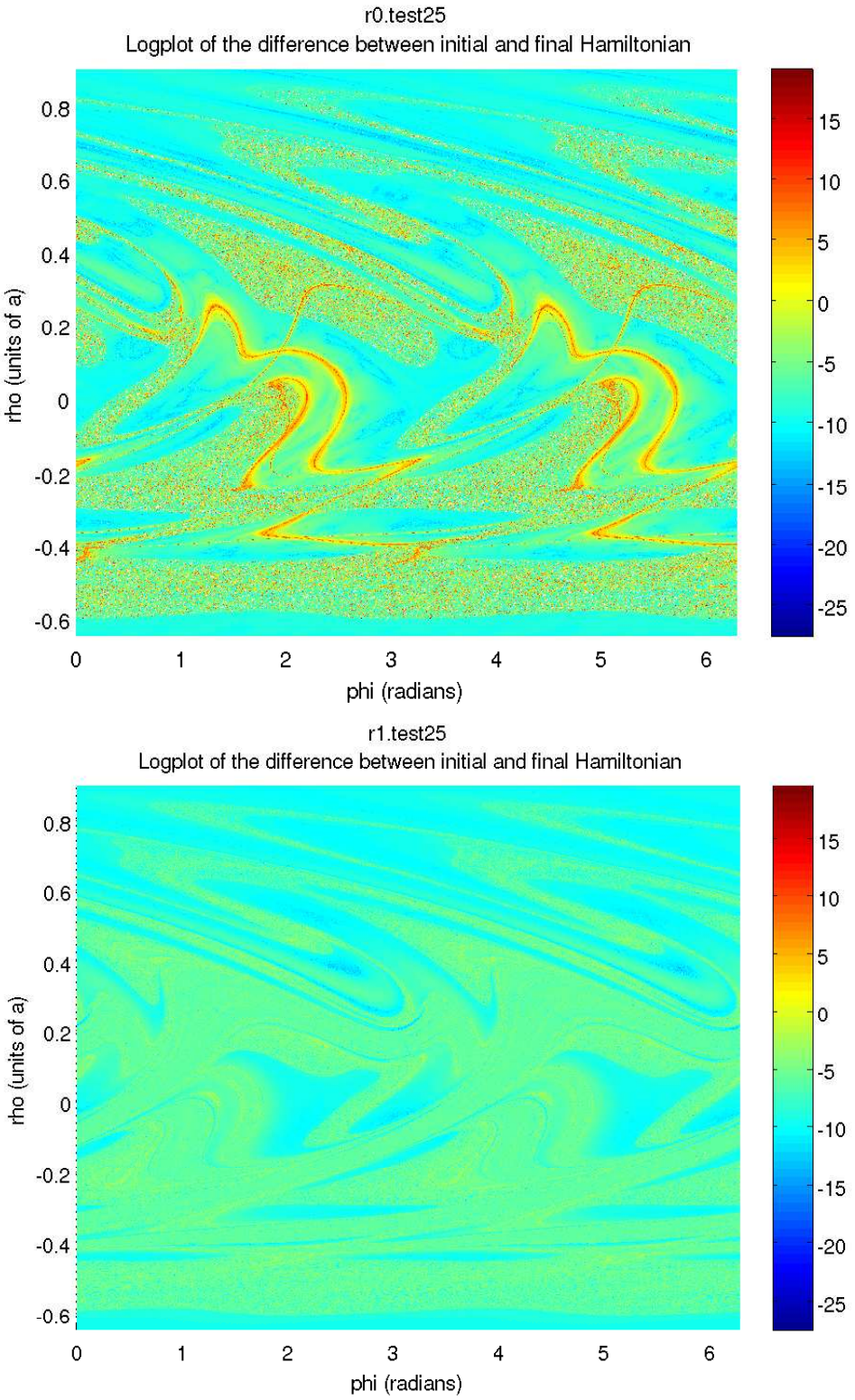


**Figure 3.5** Logplots of the change in the Hamiltonian of the Newtonian approximation (top) and the PPN1 approximation (bottom) across all relevant parameter space.

approximation. The scale shows that in almost every instance the log of the difference is negative, or the numerical differnce is less than 1. With the Hamiltonians being on the order of $3x10^6$ this level of conservation is impressive. The red lines show areas where the Hamiltonian is not conserved, but these seem to perfectly correlate with known errors and are therefore more evidence to the accuracy of our simulations.

# Chapter 4

# Pretty Pictures

## 4.1 What You Will See

The following graphs can be seen as mapping the chaos of the three body problem. The basic thing is that each pixel is a simulation. You can see the step size between pixels in the title of each graph. The graphs are labeled as belonging to the Newtonian or the PPN1 approximation. The colors represent which of the three bodies escapes from the system. Brown is the incoming, orange and green are the two parts of the binary, dark blue is where LSODA breaks down, and light blue is where runs didn't finish due to time constraints.

## 4.2 The Big Picture

Fig. 4.1 gives an overview of what we are looking at. $\phi$ ranges from 0 to $2\pi$, and $\rho$ varies from $-6.5a$ to $9a$ where $a$ is the radius of the binary. $\phi$ covers the range of distinct positions available to the binary. The range of $\rho$ reflects that at a certain distance the third body no longer interacts significantly with the binary as can be

noted from the brown bands at the top and bottom of the graphs.

The difference in magnitude between the positive and negative values of $\rho$ can be explained by the direction of rotation of the binary. In the negative direction the incoming body is moving opposite the binary and therefore has a relatively brief interaction period. In the positive direction the incoming body moves with the binary and so at the same distance from the binary there is a longer interaction period than on the negative side. This may also explain the spoon-like shapes that come in from the top. It is likely that these represent initial parameters where the incoming body passes between the binary and is able to take an energy boost from following the leading star and then using that extra energy to get thrown even when passing within $2\frac{3}{8}$ radii of the center of the binary, the approximate bottom edge of the spoon. If the brown eye below the spoon is from the same phenomenon, then using this same technique the incoming passes within 2 radii of the binary center without becoming entangled.

The large smooth regions of the pictures represent simple behavior where the third body either flies past, or takes the place of one of the binary pair in what is termed an exchange [7]. The speckled areas are much more interesting. These areas have more complex interactions where the three bodies are often bound for a time before one is cast out. The repeated interactions make them much more susceptible to non-linear effects [7].

It is important to note that there is a shift of just under one radian to the the left between the Newtonian and PPN1. This may be due to the same phenomenom that causes elliptical orbits to precess when simulated using relativity.

The dark blue lines are regions where the integrator gave up and spit out an error. They are particularly interesting when matched up with the PPN1. The rivers and new structures that show up in PPN1 often follow these error lines. These lines are

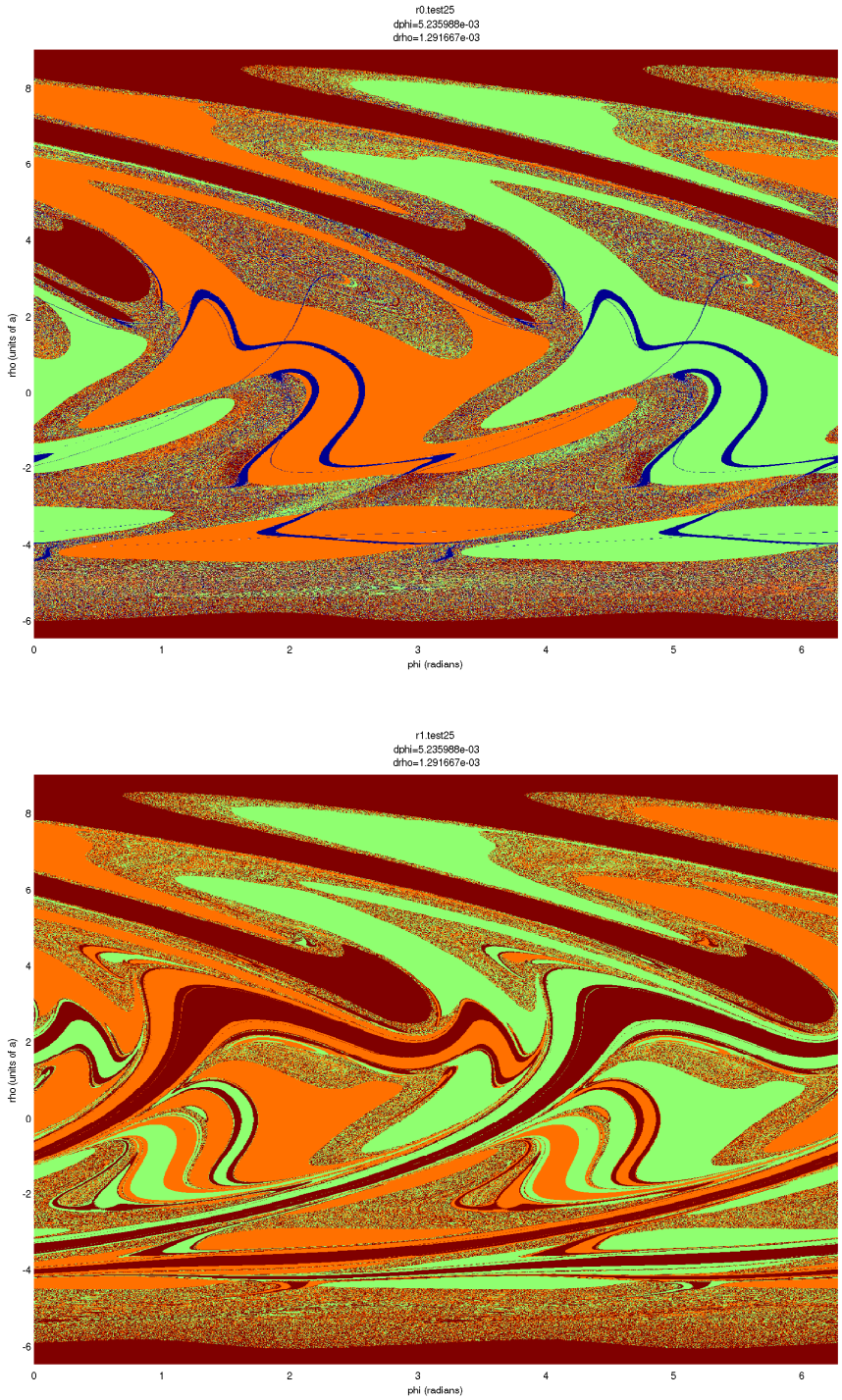


**Figure 4.1** Initial $\rho$ and $\phi$ against which body is ejected for all relevant parameter space for Newtonian (top) and PPN1 (bottom) gravity with colors representing the different bodies.

probably due to close interactions of at least two of the bodies. If they are due to such interactions, then they violate the PPN assumptions of $\frac{v^2}{c^2} \ll 1$ and $|\Phi| \ll 1$. It is also likely that such passes are not physical and would in reality be a merger or collision, but since we are using point masses they continue in the simulation until the integrator can no longer handle them. The number of initial conditions that end in "errors" is reduced from over 120,000 in the Newtonian approximation to less than 30 in the PPN1 approximation for the shown set of simulations.

## 4.3 Looking Closer

Figs. 4.2- 4.4 show progressively closer views of the bottom left of the total parameter space. One of the things that is immediately apparent is that in areas that appear to be totally chaotic, order appears. As we continue to look closer more order appears and we begin to see self-similar patterns definitive of fractals.

In the last figure, 4.5, the zoom is less drastic to allow some features to be visible in both. In particular, a focus on the blue error bands in the Newtonain approximation can be seen to match with some new rivers of chaos in the PPN1 approximation. This is easiest to see by imagining the thick blue error spike in the Newtonian approximation to be moved to the left by a little more than 1 radian and overlapping it with the brown and green hill on the far left of the PPN1 approximation. The correlation between the error lines and the rivers of chaos are likely due to the origin of said error lines. Since they are likely due to extremely close interactions of at least two of the bodies it would make sense that in the vicinity of these areas new structures would emerge due to stronger effects of relativity.

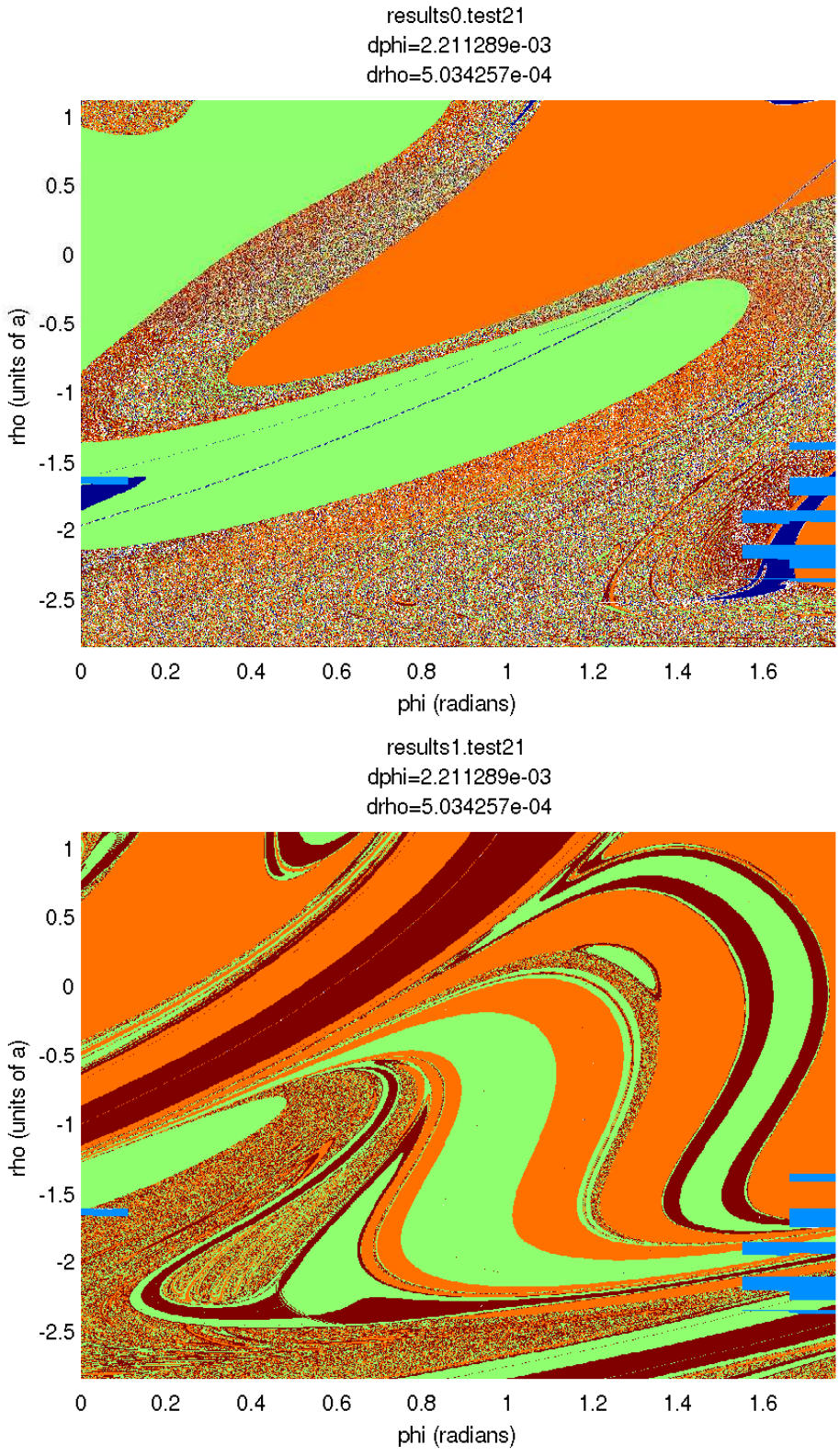


**Figure 4.2** Detail of the Newtonian approximation (top) and PPN1 approximation (bottom).

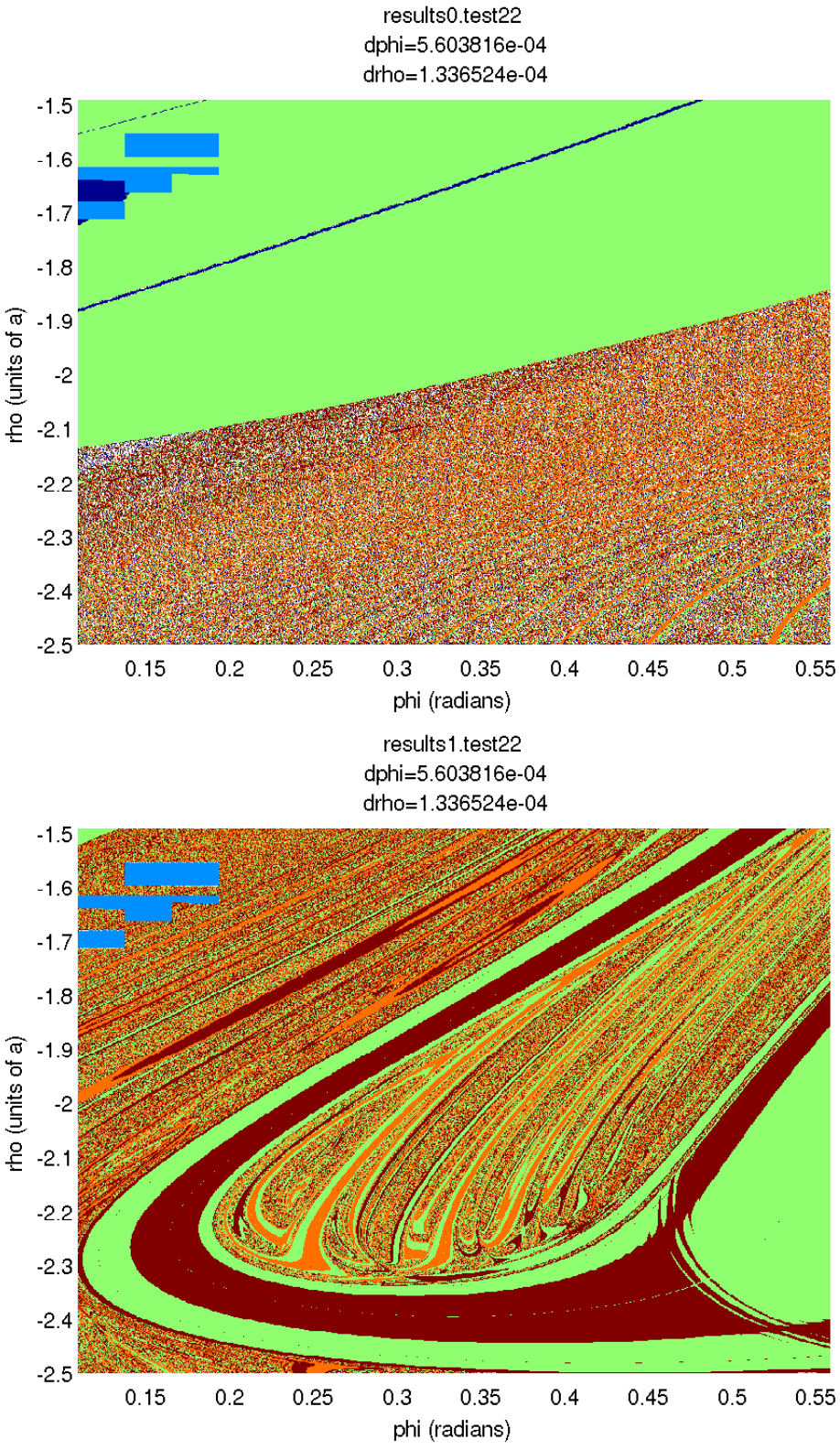


**Figure 4.3** Closer views of the Newtonian approximation (top) and PPN1 approximation (bottom) showing fine structure.

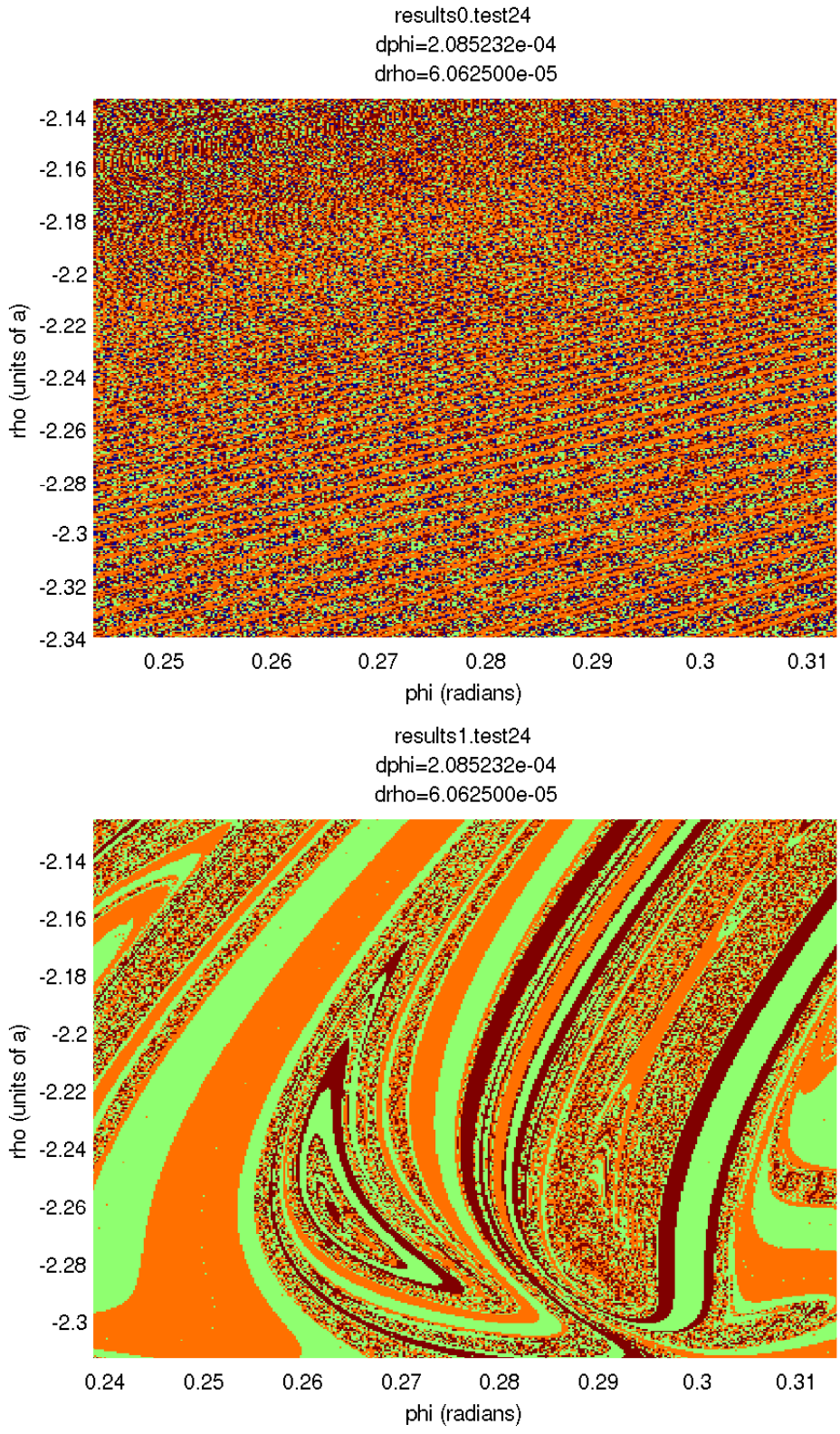


**Figure 4.4** By zooming in on the Newtonian figure (top) we can see different types of fine structure between the top and bottom. The self-similar patterns are particularly apparent in the zoom of the PPN1 figure (bottom).

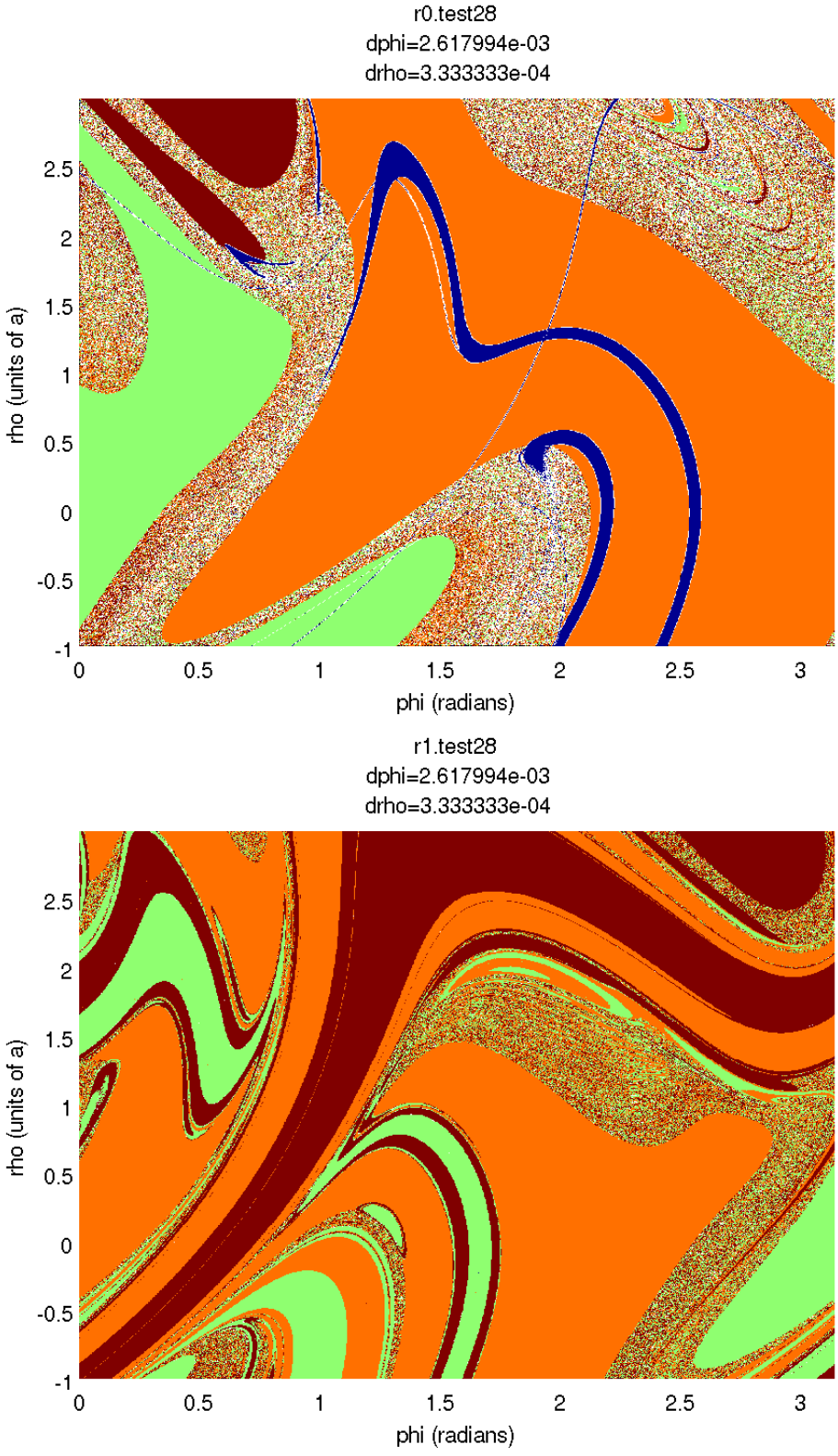


**Figure 4.5** A zoom in on the Newtonain approximation (top) and the PPN1 approximation (bottom) to allow structural comparisons between the two.

# Chapter 5

# Conclusion

## 5.1 Summary

Three-body problems are everywhere, even if we can usually avoid thinking about them. From subatomic particles to distant star systems and even to our own Solar Sytem these kind of interactions make up our world. They are difficult to study though. The Newtonian three-body problem has been studied since it was found to be chaotic by Poincaré in the late 1800's. Due to the added complexity relativity, very little has been done to combine the two areas of research. This research takes the three-body problem and examines the effects of the first order Post-Newtonian corrections across a specific range of initial conditions. The experimental simulation undertaken in this study is specifically that of a binary with a third body entering from infinity. The three objects are constrained to a plane, have equal masses, and the initial angle of the binary and the impact parameter of the third body are varied across all relevant parameter space to give an idea of both the chaotic and non-chaotic regions of interaction. I record which body escapes and graph it in relation to the initial conditions of the angle and impact parameter. I found that the general patterns

of chaotic and non-chaotic regions were maintained, though distorted. New regions of alternating chaos and order were introduced, and many orderly areas were cut across with bands of new features. It is worth noting that the number of simulations that returned as being impossible in the Newtonian approximation were reduced almost to zero in the PPN1 approximation. It also seems that overall size of the wildly chaotic regions is reduced through the relativistic corrections. Through the first order Post-Newtonian correction it appears that the three-body problem with equal masses is still chaotic. Both the Newtonian and PPN1 approximations exhibit classic fine structure and show regions of extreme sensitivity to initial conditions at least on the order of thousandths of a degree. While still chaotic, it seems that in this case the PPN1 approximation has a calming effect on the chaos.

## 5.2 Extension

This study really is just a start. As I worked through different simulations, talked with my professor, and read other works on multi-body interactions I was impressed with just how many more questions we had than answers. One of my colleagues has started working with varying the masses of the bodies. We have started running simulations that are no longer in a single plane. There are further Post-Newtonian corrections that can be implemented and studied. Taking into account mergers and collisions in accordance with the Schwarzschild radius may help to explain some observed irregularities such as the blue error lines. It may be wise to use another numerical integrator to compare results to help understand and rectify any possible aberrations inherent in numerically operating on chaotic systems. It would also be recommended to calculate the Lyapunoz constants for different regions to help quantify the chaos.

# Bibliography


[1] J. J. Lissauer, "Chaotic motion in the Solar System," Rev. Mod. Phys. **71,** 835–845 (1999).

[2] P. Cvitanović, R. Artuso, R. Mainieri, G. Tanner, and G. Vattay, *Chaos: Classical and Quantum* (Niels Bohr Institute, Copenhagen, 2008), http://ChaosBook.org (accessed 1 Dec. 2008).

[3] presented at the April 2008 APS meeting (St. Louis, MO, Apr. 2008).

[4] C. Misner, K. Thorne, and J. Wheeler, *Gravitation* (W. H. Freeman, 1973).

[5] C. Moore, "Braids in classical dynamics," Phys. Rev. Lett. **70,** 3675–3679 (1993).

[6] N. Murray and M. Holman, "The role of chaotic resonances in the Solar System," Nature **410,** 773–779 (2001).

[7] P. T. Boyd and S. L. W. McMillan, "Chaotic scattering in the gravitational three-body problem," Chaos **3,** 507–523 (1993).

[8] G. Schfer, "Three-body hamiltonian in general relativity," Phys. Lett. A **123,** 336–339 (1987).

[9] L. R. Petzold and A. C. Hindmarsh, "LSODA," http://netlib.org/alliant/ode/prog/lsoda.f (Accessed November 26, 2008).

# Appendix A

# mygrapher

This Matlab program takes the compiled data file and graphs it.

```
clear; %close all;
fileName0 = 'results0.test24';
fileName1 = 'results1.test24';
%fileName2 = 'presults2';

fprintf('Loading Files...\n');
Data0 = load(fileName0);
Dl0=length(Data0);

% define area
% start0=1;
% finish0=Dl0;

%insert x column, y column, and value to be measured
x0=2;
```

```
y0=1;
variable0=10;

Xmin0=min(Data0(:,x0));
Xmax0=max(Data0(:,x0));
Xsteps0=0;
Ymin0=min(Data0(:,y0));
Ymax0=max(Data0(:,y0));
Ysteps0=0;

for k0=1:Dl0
    if (Data0(k0,x0)==Xmin0)
        Ysteps0=Ysteps0+1;
    end
    if (Data0(k0,y0)==Ymin0)
        Xsteps0=Xsteps0+1;
    end
end

dx0=(Xmax0-Xmin0)/(Xsteps0-1);
dy0=(Ymax0-Ymin0)/(Ysteps0-1);
X0=Xmin0:dx0:Xmax0+dx0;
Y0=Ymin0:dy0:Ymax0+dy0;
Z0=zeros(length(Y0),length(X0));

for p0=1:Dl0
```

```
     Z0((round((Data0(p0,y0)-Ymin0)/dy0)+1),...
          (round((Data0(p0,x0)-Xmin0)/dx0)+1))=Data0(p0,variable0);
end

figure
surf(X0,Y0,Z0)
view([0,90])
shading flat
axis([Xmin0 Xmax0 Ymin0 Ymax0])
xlabel('phi (radians)');ylabel('rho (units of a)');
topline0=sprintf('%s\n dphi=%d\n drho=%d',fileName0,dx0,dy0);
title(topline0)
% shading interp
% colormap bone


fprintf('Loading Files...\n');
Data1 = load(fileName1);

%insert x column, y column, and value to be measured
x1=x0;
y1=y0;
variable1=variable0;

Xmin1=min(Data1(:,x1));
Xmax1=max(Data1(:,x1));
```

```
Xsteps1=0;
Ymin1=min(Data1(:,y1));
Ymax1=max(Data1(:,y1));
Ysteps1=0;
Dl1=length(Data1);

for k1=1:Dl1
    if (Data1(k1,x1)==Xmin1)
        Ysteps1=Ysteps1+1;
    end
    if (Data1(k1,y1)==Ymin1)
        Xsteps1=Xsteps1+1;
    end
end

dx1=(Xmax1-Xmin1)/(Xsteps1-1);
dy1=(Ymax1-Ymin1)/(Ysteps1-1);
X1=Xmin1:dx1:Xmax1+dx1;
Y1=Ymin1:dy1:Ymax1+dy1;
Z1=zeros(length(Y1),length(X1));
%
for p1=1:Dl1
     Z1((round((Data1(p1,y1)-Ymin1)/dy1)+1),...
          (round((Data1(p1,x1)-Xmin1)/dx1)+1))=Data1(p1,variable1);
end
```

```
figure
surf(X1,Y1,Z1)
view([0,90])
shading flat
axis([Xmin1 Xmax1 Ymin1 Ymax1])
xlabel(‘phi (radians)’);ylabel(‘rho (units of a)’);
topline1=sprintf(‘%s\n dphi=%d\n drho=%d’,fileName1,dx1,dy1);
title(topline1)
%colormap bone$
```

# Appendix B

# grapherror

This is a very similar program to **mygrapher** but graphs the conservation of the Hamiltonian.

```
clear; close all;
fileName0 = 'results0.ctest18';
fileName1 = 'results1.ctest18';
%fileName2 = 'presults2';

fprintf('Loading Files...\n');
Data0 = load(fileName0);
Dl0=length(Data0);

% %define area
% start0=1;
% finish0=Dl0;

%insert x column, y column, and value to be measured
```

```
x0=2;
y0=1;
variable0_1=14;
variable0_2=15;

Xmin0=min(Data0(:,x0));
Xmax0=max(Data0(:,x0));
Xsteps0=0;
Ymin0=min(Data0(:,y0));
Ymax0=max(Data0(:,y0));
Ysteps0=0;

for k0=1:Dl0
    if (Data0(k0,x0)==Xmin0)
        Ysteps0=Ysteps0+1;
    end
    if (Data0(k0,y0)==Ymin0)
        Xsteps0=Xsteps0+1;
    end
end

dx0=(Xmax0-Xmin0)/(Xsteps0-1);
dy0=(Ymax0-Ymin0)/(Ysteps0-1);
X0=Xmin0:dx0:Xmax0+dx0;
Y0=Ymin0:dy0:Ymax0+dy0;
Z0=zeros(length(Y0),length(X0));
```

```
%
for p0=1:Dl0
     Z0((round((Data0(p0,y0)-Ymin0)/dy0)+1),...
          (round((Data0(p0,x0)-Xmin0)/dx0)+1))...
          =log(abs(Data0(p0,variable0_1)-Data0(p0,variable0_2))+1E-12);
end

figure
surf(X0,Y0,Z0)
view([0,90])
shading flat
axis([Xmin0 Xmax0 Ymin0 Ymax0])
xlabel('phi (radians)');ylabel('rho (units of a)');
topline0=sprintf('%s\n Logplot of the difference between initial and final Hami
title(topline0)
% shading interp
% colormap bone

fprintf('Loading Files...\n');
Data1 = load(fileName1);
Dl1=length(Data1);

% %define area
% start1=1;
% finish1=Dl0;
```

```
%insert x column, y column, and value to be measured
x1=2;
y1=1;
variable1_1=14;
variable1_2=15;

Xmin1=min(Data1(:,x1));
Xmax1=max(Data1(:,x1));
Xsteps1=0;
Ymin1=min(Data1(:,y1));
Ymax1=max(Data1(:,y1));
Ysteps1=0;

for k1=1:Dl1
    if (Data1(k1,x1)==Xmin1)
        Ysteps1=Ysteps1+1;
    end
    if (Data1(k1,y1)==Ymin1)
        Xsteps1=Xsteps1+1;
    end
end

dx1=(Xmax1-Xmin1)/(Xsteps1-1);
dy1=(Ymax1-Ymin1)/(Ysteps1-1);
X1=Xmin1:dx1:Xmax1+dx1;
Y1=Ymin1:dy1:Ymax1+dy1;
```

```
Z1=zeros(length(Y1),length(X1));
%
for p1=1:Dl1
     Z1((round((Data1(p1,y1)-Ymin1)/dy1)+1),...
          (round((Data1(p1,x1)-Xmin1)/dx1)+1))...
          =log(abs(Data1(p1,variable1_1)-Data1(p1,variable1_2))+1E-12);
end

figure
surf(X1,Y1,Z1)
view([0,90])
shading flat
axis([Xmin1 Xmax1 Ymin1 Ymax1])
xlabel('phi (radians)');ylabel('rho (units of a)');
topline1=sprintf('%s\n Logplot of the difference between initial and final Hami
title(topline1)
% shading interp
% colormap bone
```

# Appendix C

# e7

This Matlab program takes the output data file from a modified run of nbodyPN that tracks the motion of a single simulation. This data is then visually rendered to facilitate comparisons.

```
clear; close all;
z=1:100001;
load e7_1;
d=e7_1';
x=d(1,:);
xb=x(1,1:1100);
xe=x(1,98901:100001);
y=d(2,:);
yb=y(1,1:1100);
ye=y(1,98901:100001);

load e7_2;
i=e7_2';
```

```
xi=i(1,:);

xib=xi(1,1:84);

xie=xi(1,99917:100001);

yi=i(2,:);

yib=yi(1,1:84);

yie=yi(1,99917:100001);


figure

plot3(x,y,z,‘r-’)

hold on

plot3(xi,yi,z,‘b-’)

axis([-.8 .8 -.8 .8 0 100001])

hold off


figure

plot(xb,yb,‘b-’)

hold on

plot(xe,ye,‘r-’)

plot(xib,yib,‘b-’)

plot(xie,yie,‘r-’)

hold off
```